



**HAL**  
open science

## Influence of consolidation process on voids and mechanical properties of powdered and commingled carbon/PPS laminates

Julien Patou, Rébecca Bonnaire, Emmanuel de Luycker, Gérard Bernhart

### ► To cite this version:

Julien Patou, Rébecca Bonnaire, Emmanuel de Luycker, Gérard Bernhart. Influence of consolidation process on voids and mechanical properties of powdered and commingled carbon/PPS laminates. *Composites Part A: Applied Science and Manufacturing*, 2019, 117, p.260-275. 10.1016/j.compositesa.2018.11.012 . hal-01943849

**HAL Id: hal-01943849**

**<https://imt-mines-albi.hal.science/hal-01943849>**

Submitted on 11 Jan 2019

**HAL** is a multi-disciplinary open access archive for the deposit and dissemination of scientific research documents, whether they are published or not. The documents may come from teaching and research institutions in France or abroad, or from public or private research centers.

L'archive ouverte pluridisciplinaire **HAL**, est destinée au dépôt et à la diffusion de documents scientifiques de niveau recherche, publiés ou non, émanant des établissements d'enseignement et de recherche français ou étrangers, des laboratoires publics ou privés.

# Influence of consolidation process on voids and mechanical properties of powdered and commingled carbon/PPS laminates

Julien Patou<sup>a,\*</sup>, Rébecca Bonnaire<sup>a</sup>, Emmanuel De Luycker<sup>b</sup>, Gérard Bernhart<sup>a</sup>

<sup>a</sup> Institut Clément Ader (ICA), Université de Toulouse, CNRS, Mines Albi, UPS, INSA, ISAE-SUPAERO, Campus Jarlard, 81013 Albi CT Cedex 09, France

<sup>b</sup> Laboratoire Génie de Production, Université de Toulouse, INP-ENIT, Tarbes, France

## ABSTRACT

### Keywords:

- A. Thermoplastic resin
- B. Porosity
- C. Mechanical properties
- D. Microstructural analysis
- E. Consolidation

Relations between autoclave consolidation process, microstructure and mechanical properties of thermoplastic composite laminates were investigated. For this purpose, two different carbon fibers/PPS semi-pregs were used for laminate manufacturing: a powdered fabric and a commingled fabric with stretch broken fibers. Laminates with  $[0^\circ]_6$  stacking sequence were consolidated in autoclave. Several consolidation levels were established by varying process parameters which are external pressure, vacuum level and consolidation duration. Microstructural characterization was performed by using matrix digestion and CT-scanning to identify void content and morphology. Laminate mechanical properties in tensile, bending, compressive and interlaminar shear were also assessed. External pressure increase by 0.5 MPa leads to void content reduction of 2.1% for powdered system and 5.4% for commingled system. The rising consolidation duration contributes slightly to void content decrease. Bending and interlaminar failure stress are the most sensitive to void level with a dependency on void size and location. Results acquired allow to identify main settings for optimized consolidation cycles which could be used for thermoplastic composite part manufacturing with complex shape.

## 1. Introduction

Manufacturing structural or semi-structural composite parts by consolidation was introduced in the aeronautical industry in order to answer mainly weight reduction requirements. Use of thermoplastic resins for composite manufacturing offers new significant advantages compared to thermoset ones as no shelf life, no volatile emissions, short forming duration for example using thermo-stamping processes and welding capabilities; the two later aim to respond to manufacturing cost reduction issues. However, thermoplastic viscosity at processing temperature ranges from 100 Pa s to 1000 Pa s whereas thermoset viscosity does not exceed 10 Pa s [1]. As a consequence, matrix impregnation inside reinforcement bundles is difficult and voids may appear when processing the laminate. Moreover, manufacturing thermoplastic composite parts encounter limitations related to the high-processing temperatures and to draping of complex 3D shape parts [2].

It is known that autoclave consolidation is well adapted to manufacture complex shape composite parts. Combined with an appropriate process cycle selection and bagging strategy, it allows to minimize void level and maximize mechanical properties. When addressing semi-structural parts like air conditioning volutes and plenums, functional requirements are fulfilled even if void level is as high as 7.0%. Relaxing

this level may also relax manufacturing constraints and contribute to manufacturing cost decrease. Nevertheless, such a high level can only be accepted if mechanical properties are not deeply affected.

Many experimental works have investigated the relation between void content and laminate mechanical properties [3–6]; they have shown that interlaminar shear and bending rupture stresses are very sensitive even to low void level for UD laminates [7,8]. Nevertheless only a few results are reported in open literature for thermoplastic materials [2,9,7]. Moreover, they were obtained mostly on non-thermostable thermoplastic composites (PP polymers).

This paper aims to investigate the relation between autoclave consolidation parameters, void level and morphology (shape, size) and mechanical properties of C/PPS (carbon fiber with polyphenylene sulfide polymer) laminates. It addresses and compares two C/PPS laminates manufactured with two different initial semi-pregs (fiber reinforcement which is partially impregnated with the resin): a powdered fabric and a stretch broken commingled fabric. These fabrics were selected because of their relative short flow distance for the matrix to impregnate the reinforcement in comparison with others technics like “film stacking”. In order to get a better understanding of microstructure impact on laminates mechanical behaviour, void characterisation was performed using X-ray computed tomography.

\* Corresponding author.

E-mail address: [julien.patou@mines-albi.fr](mailto:julien.patou@mines-albi.fr) (J. Patou).

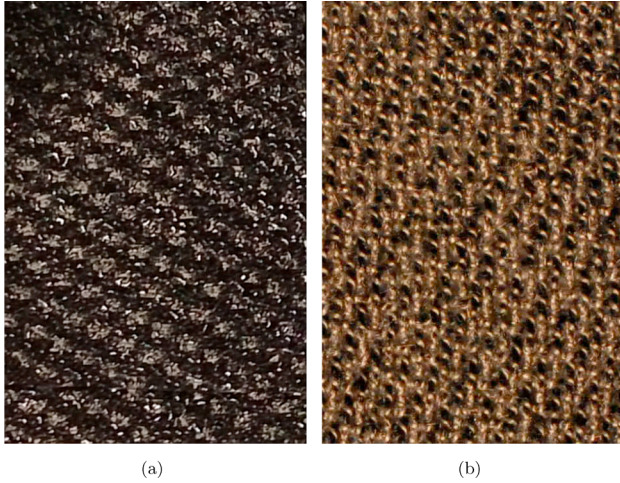


**Fig. 1.** Semi-pregs: (a) Carbon fiber powdered fabric - Pipreg®- Porcher Industries (b) Carbon fiber commingled fabric - TPFL®- Schappe Techniques. (For interpretation of the references to colour in this figure legend, the reader is referred to the web version of this article.)

**Table 1**  
Fabrics properties.

		Powdered fabric <i>Porcher Industries</i>	Commingled <i>Schappe Techniques</i>
Type		Pipreg®3106-P23	TPFL®90163P
Weave		5 H Satin	5 H Satin
Structure		3 K HS	3 K HS
Dry fabric areal weight	[g/m <sup>2</sup> ]	285	281
Polymer areal weight	[g/m <sup>2</sup> ]	216	188
Fiber density	[g/cm <sup>3</sup> ]	1.77	1.75
Matrix density	[g/cm <sup>3</sup> ]	1.35	1.41
Theoretical ply thickness	[mm]	0.317	0.297
fully consolidated	[%]	51	55
Fiber volume fraction			

## 2. Materials and manufacturing conditions

### 2.1. Materials

Two C/PPS (carbon fiber with polyphenylene sulfide polymer) semi-pregs were investigated: a 5H satin powdered impregnated fabric (Pipreg® from Porcher Industries in Fig. 1(a)) and a 5H satin commingled fabric with stretch-broken carbon fibers (TPFL® from Schappe

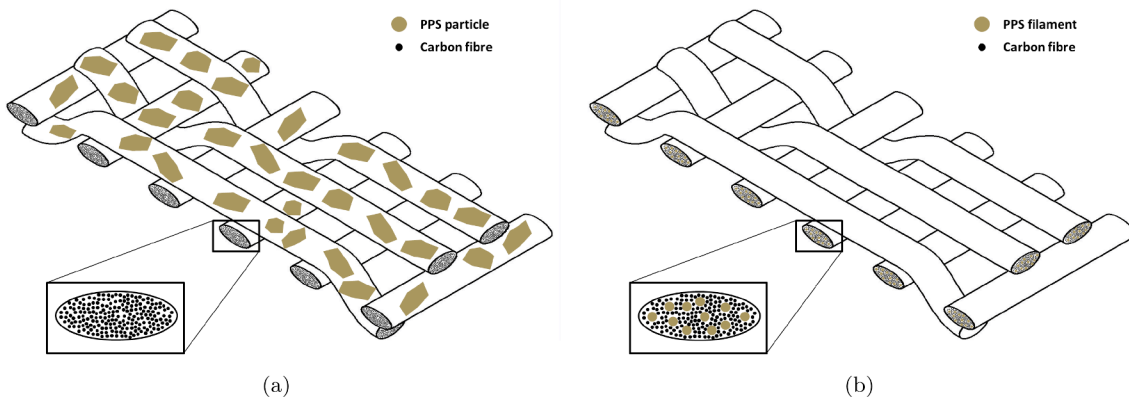


**Fig. 2.** Structural aspect of the two prepreg fabrics: (a) Powdered fabric - (b) Commingled fabric. (For interpretation of the references to colour in this figure legend, the reader is referred to the web version of this article.)

Techniques in Fig. 1(b)). A detailed description of the semi-pregs is given in (Table 1).

Both fabrics were studied because of the “short” flow distance required for the matrix to fully impregnate the reinforcement (Fig. 2). For powdered fabrics, the polymer is applied in the form of droplets to the reinforcement surface so as to foster significantly the interlayer impregnation. For the commingled one, the polymer is deeply integrated inside the bundles as polymer filaments (typically 20.0 μm diameter) to ensure intra bundle impregnation. This later semi-preg is a deformable fabric that can be easily used to drape complex shape parts [10,11].

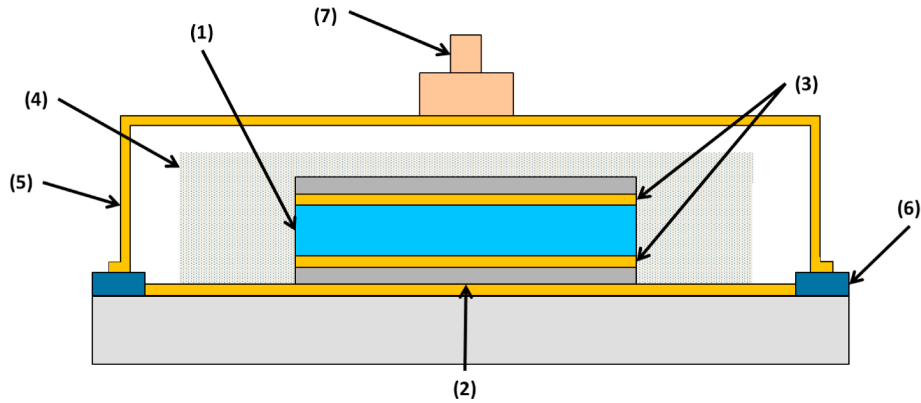
For a given consolidation cycle, these two semi-pregs are expected not to give the same mechanical properties. This may be explained by the void content differences present in the laminates.

### 2.2. Laminate consolidation

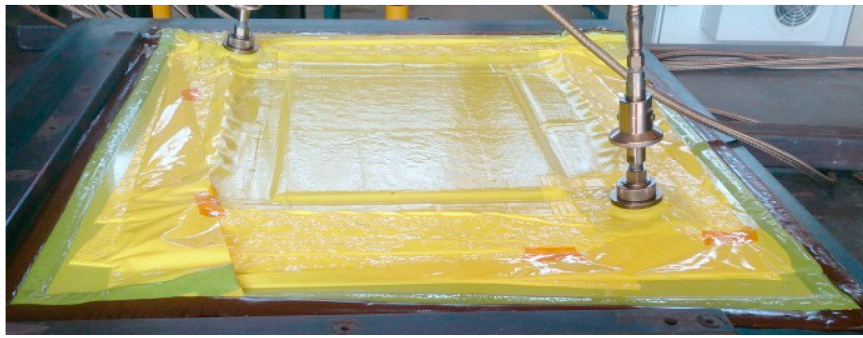
For each type of semi-preg, 6 layers were used with a stacking sequence  $[0^0]_6$  ( $0^0$  correspond to the warp direction of the 5 H Satin weave) to obtain sheets with a final thickness of  $1.9 \pm 0.1$  mm for the powder fabric and  $1.8 \pm 0.1$  mm for the commingled one. A cross-section of vacuum bagging setup is shown in Fig. 3. The semi-preg layers (1) were inserted between two Kovar plates (2) in order to obtain laminates with flat surfaces. A polyimide film (3) was used as separator between laminate and Kovar plates. Breather (Airweave UHT 800 Airtech) (4) on the lateral border of the laminate and on the upper surface of the Kovar plate allowed the evacuation of trapped air bubbles during consolidation. Vacuum-bagging film (5) (PTFE film VB-3) was used with tape (6) (A-800-3G - Airtech) to ensure the sealing. Most research in thermoplastic prepreg consolidation was done with polyimide film as vacuum bagging [12]. Finally, trapped air was evacuated by a valve (VAC VALVE 409SS HTR Airtech) settled on the vacuum bagging (7). All metallic parts and polyimide film in contact with the laminate were treated with a release agent (Frekote 700N).

In order to reach different consolidation levels, two processing devices were used for the  $400 \times 300$  mm<sup>2</sup> sheet manufacturing: an autoclave (Scholtz  $\phi = 1.0$  m; L = 1.5 m) and an oven (Nabertherm l = 1.2 m - L = 2.0 m - H = 2.0 m). Processing parameters which are consolidation times, external pressure and vacuum pressure conditions are reported in Table 2. All cycles were performed with a consolidation temperature of 310 °C.

Fig. 4 shows typical thermal and pressure cycles applied for composite sheet manufacturing. Autoclave and oven temperature profiles are close to the expected cycle as the temperature regulation thermocouple is located on the mold. Consolidation cycles were defined in order to be able to analyse the effects of external pressure, vacuum level and consolidation time on the composite sheet microstructure. Consolidation pressure effect was tested with five levels: no external



(a) Cross section of the vacuum bagging setup



(b) Vacuum bagging with VB-3 film

**Fig. 3.** Vacuum bagging setup for autoclave thermoplastic consolidation. (For interpretation of the references to colour in this figure legend, the reader is referred to the web version of this article.)

pressure, 0.5 MPa, 1.0 MPa, 1.2 MPa and 1.7 MPa. Consolidation duration impact was assessed by varying the duration of the constant temperature step from 10 min to 25 min. Maximum pressure reached inside the bagging is indicated in Table 2 for each consolidation cycle. Internal pressure losses inside the bagging, also indicated in this table, are not controlled from one test to another. However, they are measured and used for the discussion. These values depend on the choice of vacuum bagging materials and pressure application conditions: no external pressure, application of the maximal external pressure during the whole process, only during the consolidation step at 310 °C or in a two-step pressure cycle (first compaction at 0.3 MPa until [220–240 °C] before using the final consolidation pressure). For some consolidation cases, vacuum was partially or totally lost during the process. It is mainly due to leaks occurring during the heating or the consolidation step. Vacuum is totally lost due to a bad adhesion of the vacuum-bagging film on the sealant tape or to film perforation in the valves area. The non-repeatability of the process is not critical. The objective was manufacturing composite part with different consolidation levels. Some improvements in the vacuum bagging preparation were done to prevent from leaks and to manufacture composite laminates with the lowest void content.

### 3. Experimental testing procedures

#### 3.1. Specimen machining

Samples used for laminate characterization were cut by water jet cutting (MACHINE FLOW MACH4-C). For each composite sheet, eight tensile samples of  $250 \times 25 \times 2 \text{ mm}^3$ , five compressive samples of  $110 \times 10 \times 2 \text{ mm}^3$ , five inter-laminar shear testing samples of

**Table 2**

Laminate processing cycles - (A) for powdered fabrics and (B) for commingled fabrics

Id.	$P_{vacuum}$ level [MPa]	Maximum internal pressure [MPa]	Consolidation duration [min]	$P_{Ext}$ [MPa]	Pressure conditions application
A1	-0.07	+0.06	10	0.5	All along the process
A2	-0.07	+0.06	10	1.2	At $T \sim 290 \text{ °C}$
A3	-0.07	-0.01	10	0.5	First compaction of 0.3 MPa
A4	-0.04	Lost <sup>a</sup>	20	1.7	
A5	-0.06	-0.04	10	0	N\A
A6	-0.06	-0.04	20	0	N\A
B1	-0.07	+0.06	10	0.5	All along the process
B2	-0.07	+0.06	10	1.2	
B3	-0.07	+0.06	20	0.5	
B4	-0.04	Lost <sup>a</sup>	20	1.7	First compaction of 0.3 MPa
B5	-0.08	+0.01	25	1.0	

<sup>a</sup> Internal pressure measure lost.

$100 \times 15 \times 2 \text{ mm}^3$  and 15 void assessment samples of  $20 \times 10 \times 2 \text{ mm}^3$  were machined.

#### 3.2. Void content assessment

Void level's are usually measured by optical microscopy. However, to obtain information on the whole samples, porosity level was

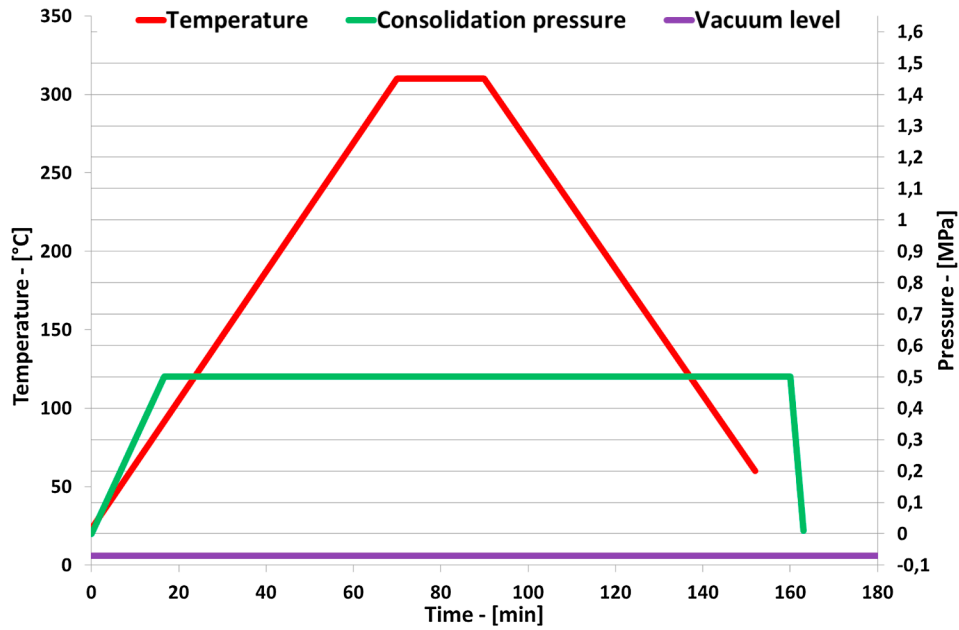


Fig. 4. Typical consolidation cycles used for laminate manufacturing. (For interpretation of the references to colour in this figure legend, the reader is referred to the web version of this article.)

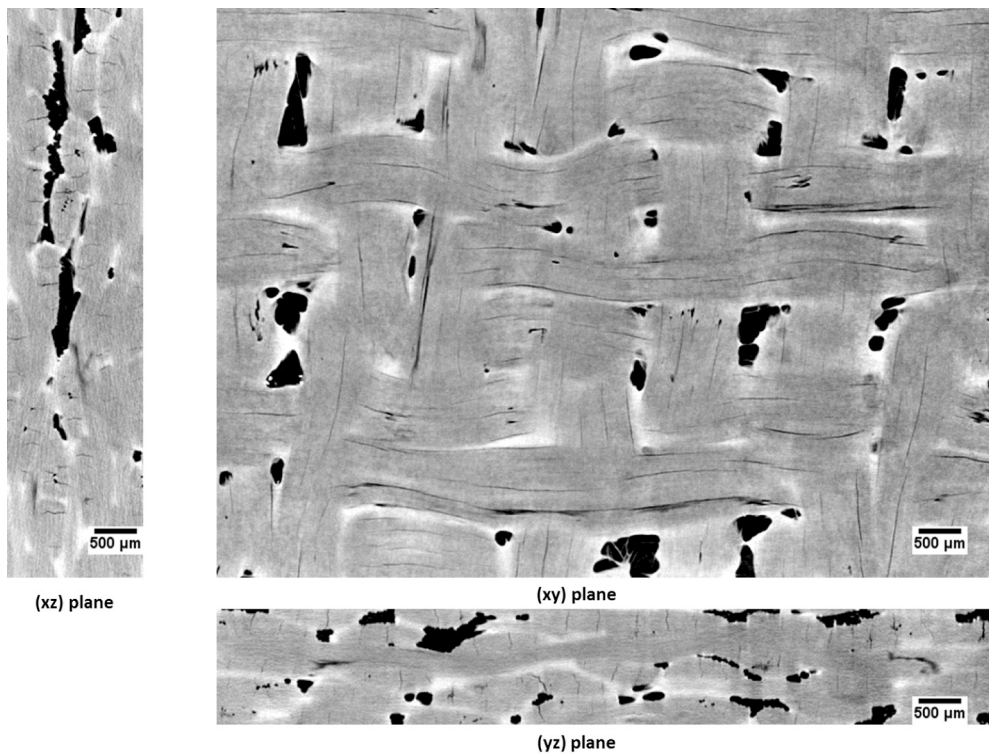


Fig. 5. 3 plane images coming from CT-scan reconstruction of a commingled sample (Sample: B3;  $V_p = 7.09\%$ ).

established firstly by matrix digestion according to NF EN 2564. A concentrated sulfuric acid solution is used to separate the fibers from the matrix. The weight of dry fibers weight are measured so as to obtain fiber volume fraction and to deduce void content. This procedure requires the knowledge of sample density using Archimedes Principle [13]. A minimum of three specimens from each laminate were analyzed to obtain an average value of void content. The mean measure uncertainty for this method is 0.89%.

### 3.3. Determination of porosity size and shape

X-ray computed tomography (CT-scanning) was performed to obtain information in terms of size and shape of voids contained inside the samples. A typical view in (xy), (yz) and (xz) planes of commingled sample (B3) is shown in Fig. 5.

The sample is represented as voxels (3D pixels) which correspond individually to the intensity of the material local density (grayscale

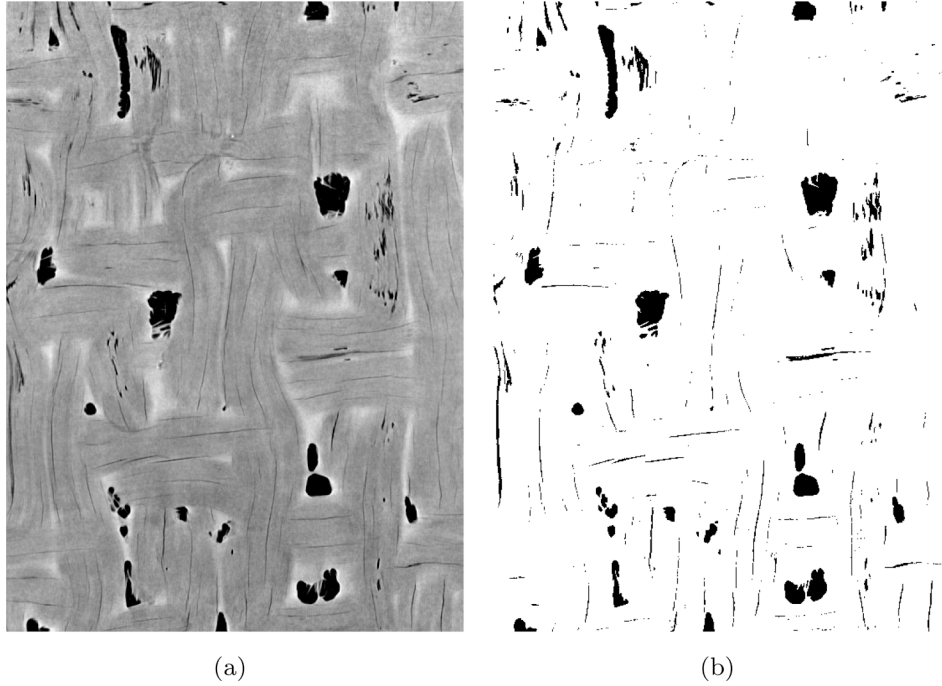


Fig. 6. Image segmentation for laminate B3: (a) 3D image coming from CT-Scan - (b) Segmented image.

value). Objects which have a low density material, such as voids, absorb fewer X-rays than a higher density material such as fiber and matrix. Consequently, in this case, porosity objects have the lowest attenuation coefficient with a grey value close to 0 (black color). On the contrary, fiber and matrix objects have a higher gray value (approaching white color for the matrix one).

All samples were analyzed with an Easytom 130 tomograph. The X-ray voltage was set to 44 kV and the power source to 181  $\mu$ A. Scan resolution, in terms of voxel size, is  $11.2 \mu\text{m} \pm 0.8 \mu\text{m}$ . Reconstructed 3D images, converted to 8-bits (greyscale value in the range [0–255]), were analyzed with post-processing software ImageJ version 1.51 [14].

In order to analyse voids within the laminates, segmentation was performed to obtain binary images allowing a clear separation between voids and fiber/matrix groups (Fig. 6). Grey threshold value, used for this image processing, was determined for each slice to take into account exposure differences of successive slices. 3D segmentation was performed with an automatic procedure implemented in Matlab® (MathWorks®).

### 3.4. Mechanical testing

Mechanical tests were performed according to the international standards: ISO 14130 for inter-laminar shear, ISO 14125 for the three points bending, ISO 527 for tensile tests and ISO 14126 for compressive tests. For each laminate, five specimens were tested except for tensile 90° where only three samples were used.

## 4. Results and discussion

### 4.1. Laminate void assessment

Results obtained for void content, fiber volume fraction and laminate thickness are reported in Table 3 and Fig. 7 for all laminates investigated. High standard deviation ( $>1.0\%$ ) are noticed for samples A1, A4 and B1. Ultrasonic inspection shows a heterogeneous distribution of the voids for these laminates and explained the high dispersion measured by CT-Scan and matrix digestion.

Table 3

Laminate ply thickness, fiber and void volume fraction

Id.	Fiber volume fraction [%]	Ply thickness [mm]	Void volume fraction [%]
A1	$51.45 \pm (3.31)$	$0.33 \pm (0.07)$	$2.46 \pm (1.30)$
A2	$49.54 \pm (0.97)$	$0.32 \pm (0.06)$	$2.45 \pm (0.17)$
A3	$50.80 \pm (0.69)$	$0.32 \pm (0.09)$	$1.55 \pm (0.67)$
A4	$59.34 \pm (2.78)$	$0.30 \pm (0.15)$	$2.27 \pm (1.71)$
A5	$50.68 \pm (1.36)$	$0.33 \pm (0.05)$	$4.57 \pm (0.67)$
A6	$51.94 \pm (0.91)$	$0.32 \pm (0.04)$	$3.43 \pm (0.53)$
B1	$55.22 \pm (2.15)$	$0.31 \pm (0.02)$	$6.02 \pm (1.11)$
B2	$54.77 \pm (0.88)$	$0.30 \pm (0.02)$	$4.06 \pm (0.70)$
B3	$54.16 \pm (2.53)$	$0.37 \pm (0.02)$	$7.09 \pm (0.78)$
B4	$49.51 \pm (0.40)$	$0.34 \pm (0.02)$	$12.11 \pm (0.81)$
B5	$55.40 \pm (0.78)$	$0.32 \pm (0.03)$	$1.65 \pm (0.30)$

#### 4.1.1. Powdered fabric laminates

For the powder fabric laminates (Pipreg®), void content obtained by matrix digestion varies from 1.50% to 4.60%. Laminates have globally the same fiber volume fraction close to 50% and the mean thickness is close to 2.0 mm. Mean ply thickness is 0.32 mm which is slightly higher than the value reported in the data sheet (0.317 mm) obtained for laminates manufactured by hot-pressing. Only specimen A4 shows values out of the range with a fiber volume fraction close to 60% that could be explained by the very high external pressure applied during consolidation (1.7 MPa) which squeezes the polymer out of the laminate. As expected the maximal void content (4.57%) is registered on laminate A5 after a consolidation duration of 10 min and without external pressure. The minimal void content (1.55%) is measured on the laminate A3 with 0.5 MPa as consolidation pressure, 10 min as consolidation duration and a low vacuum level maintained throughout the process.

Fig. 8 shows CT-scans of powdered fabric laminates for three porosity levels. According to slice analysis, two void types are identified:

- **Intra-yarn voids** have mostly a spherical aspect. These voids are

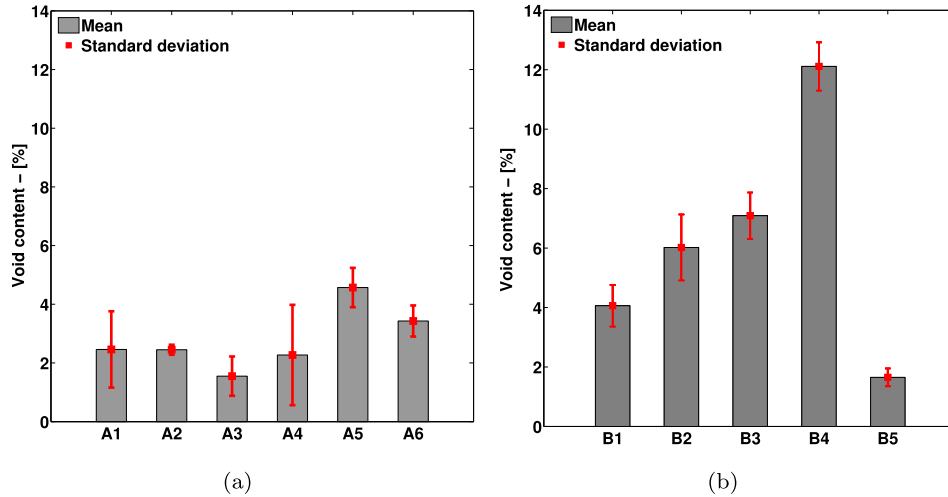


Fig. 7. Void content (matrix digestion) for (a) powdered and (b) commingled laminates. (For interpretation of the references to colour in this figure legend, the reader is referred to the web version of this article.)

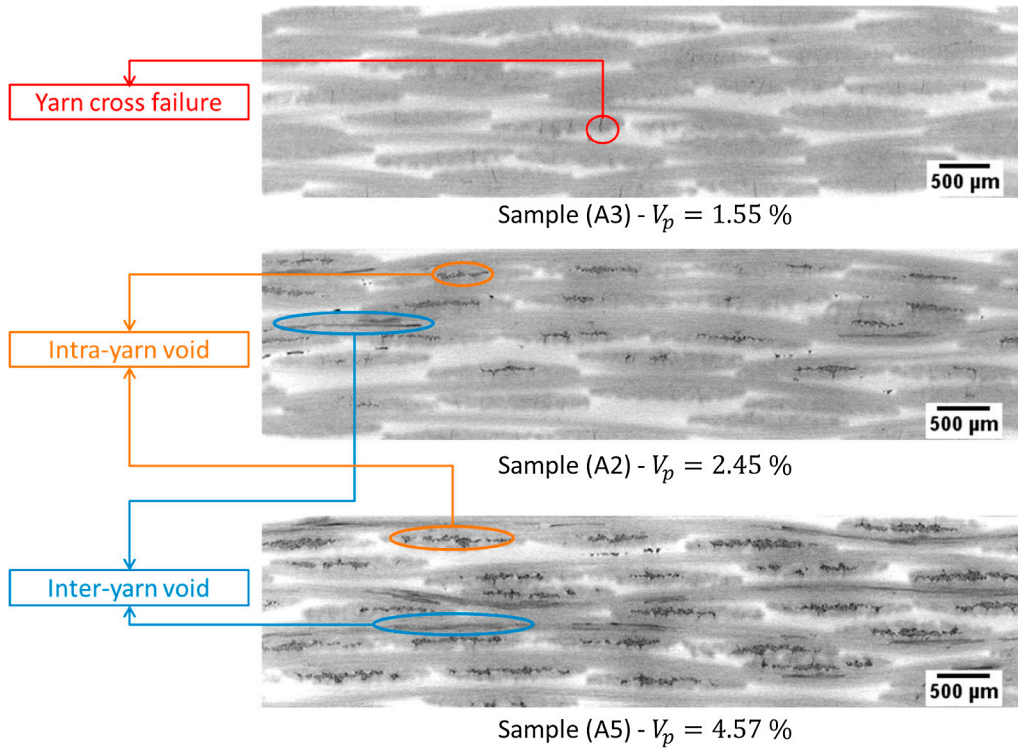


Fig. 8. CT-scans of powdered C/PPS laminates for increasing void content. (For interpretation of the references to colour in this figure legend, the reader is referred to the web version of this article.)

typical for powdered fabrics and are related to the higher impregnation length required for the polymer to reach the center of the yarn. A laminate not fully consolidated as A2 presents voids mostly located inside the yarns when compared to a fully consolidated one. In sample A5 which shows the highest void content, spherical voids are organized in clusters in each yarn and form macro-voids. The latter have an ellipsoidal shape and are oriented along the directions of the textile reinforcement.

- **Inter-yarn voids:** Found only in the sample A5, these voids are larger than the spherical ones and are located mostly between yarns or in contact to yarn surface. They also have an elongated shape and

their orientations follow the warp and weft direction of the textile reinforcement as can be seen on the 3D porosity representation of sample A5 in Fig. 9.

- **Yarn cross failure:** There are some transversal cracks detected only in sample A3.

Void area distribution for powdered laminates A3 ( $V_p = 1.55\%$ ) and A5 ( $V_p = 4.57\%$ ) are reported in Fig. 10. Results take into account the analysis of all the slices of the specimen. Two void size categories called *micro* [ $0 \mu\text{m}^2 - 6.10^3 \mu\text{m}^2$ ] and *macro-porosities* ( $> 6.10^4 \mu\text{m}^2$ ) were separated in order to help understanding void size distribution. The size

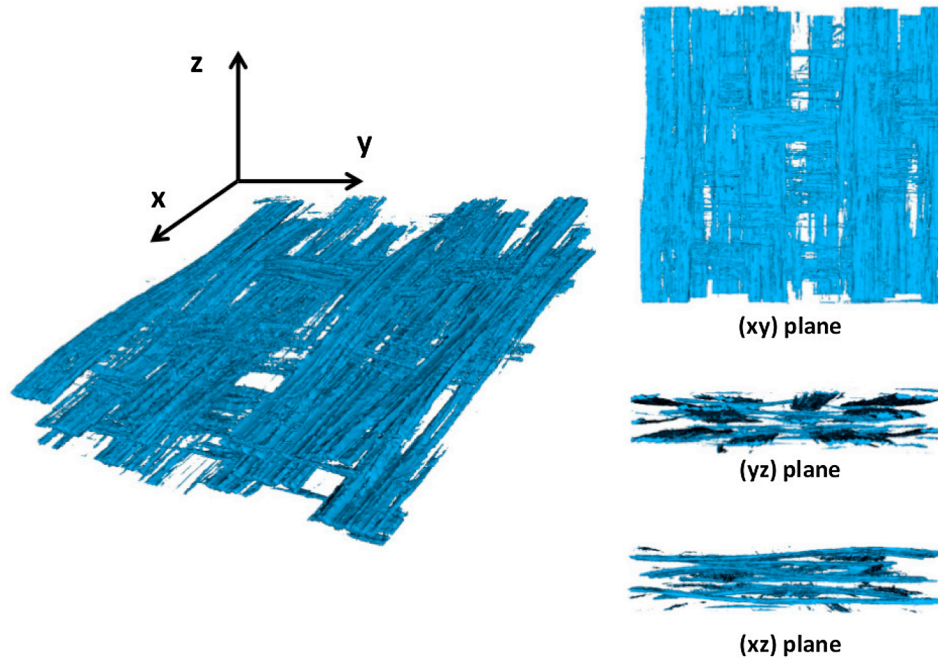


Fig. 9. 3D representation of porosities for powdered sample A5 ( $V_p = 4.57\%$ ). (For interpretation of the references to colour in this figure legend, the reader is referred to the web version of this article.)

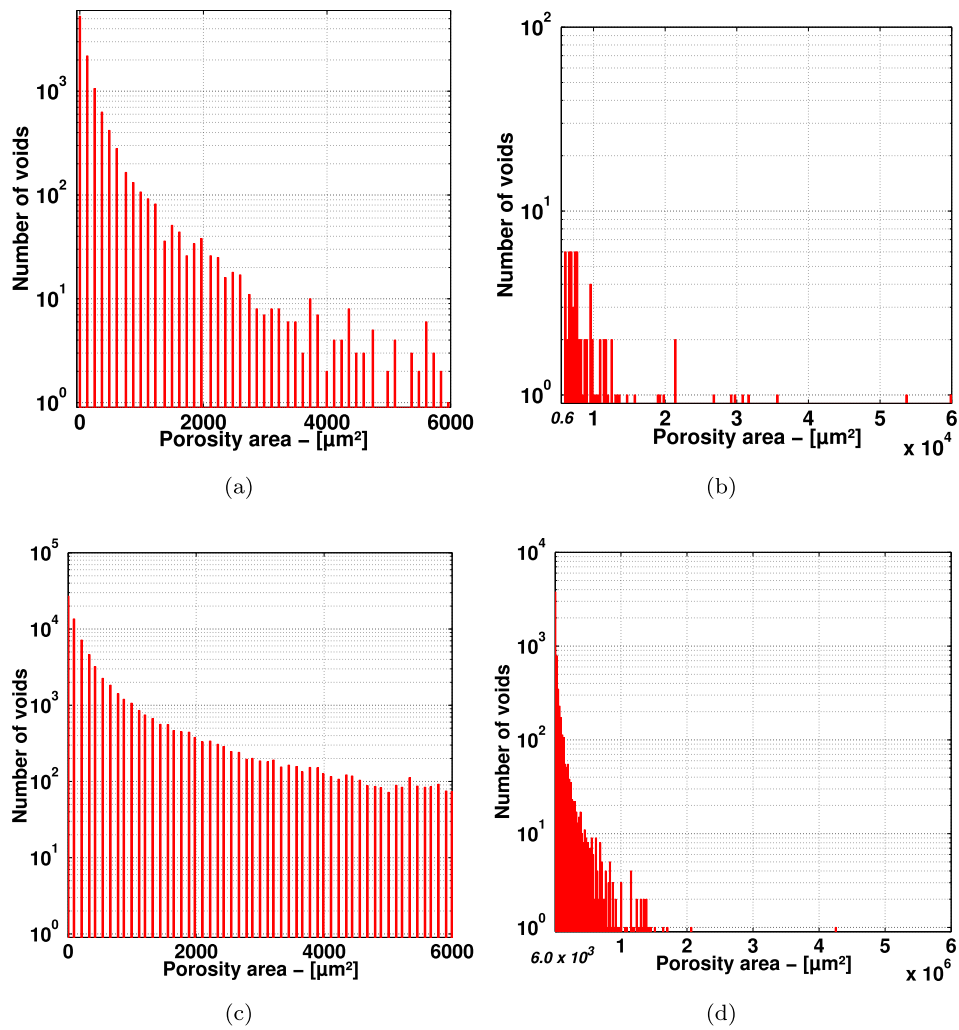


Fig. 10. Void area distribution: (a) Sample A3 - Micro-voids ( $<6.0 \times 10^3 \mu\text{m}^2$ ) - (b) Sample A3 - Macro-voids ( $>6.0 \times 10^3 \mu\text{m}^2$ ) - (c) Sample A5 - Micro-voids ( $<6.0 \times 10^3 \mu\text{m}^2$ ) - (d) Sample A5 - Macro-voids ( $>6.0 \times 10^3 \mu\text{m}^2$ ). (For interpretation of the references to colour in this figure legend, the reader is referred to the web version of this article.)

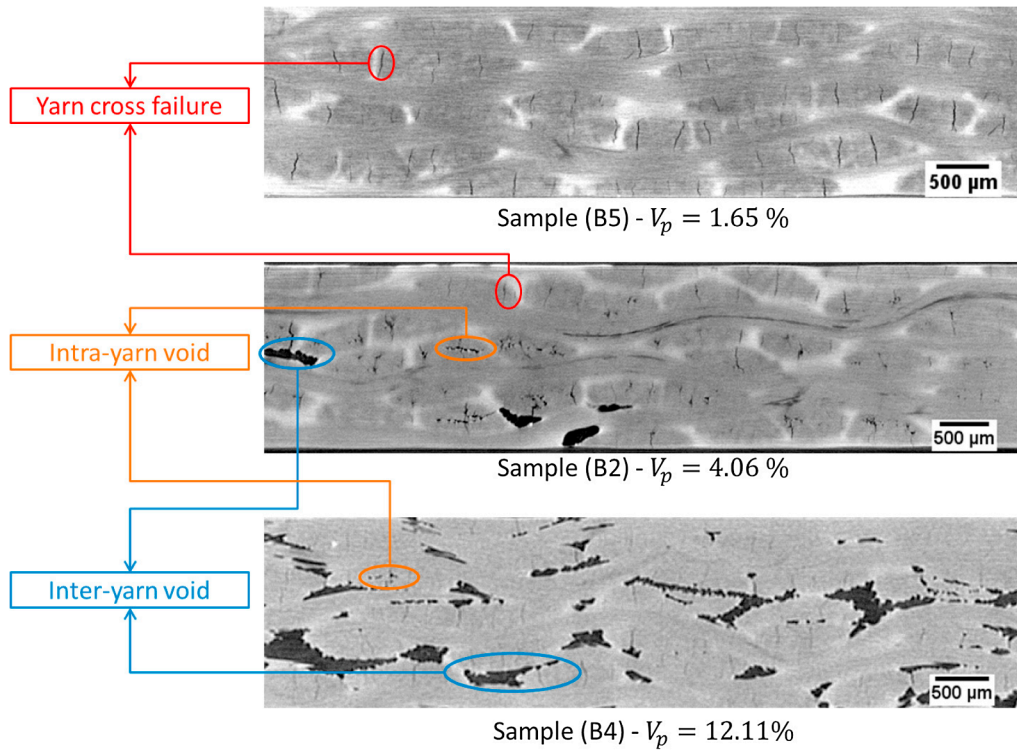


Fig. 11. CT-scans of commingled C/PPS laminate for increasing void content. (For interpretation of the references to colour in this figure legend, the reader is referred to the web version of this article.)

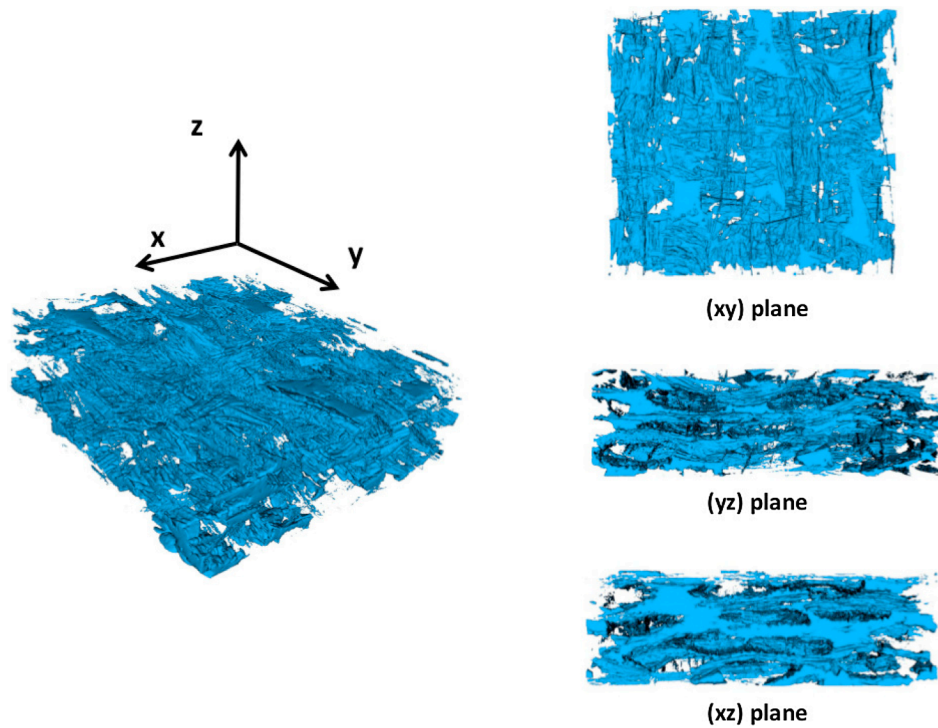
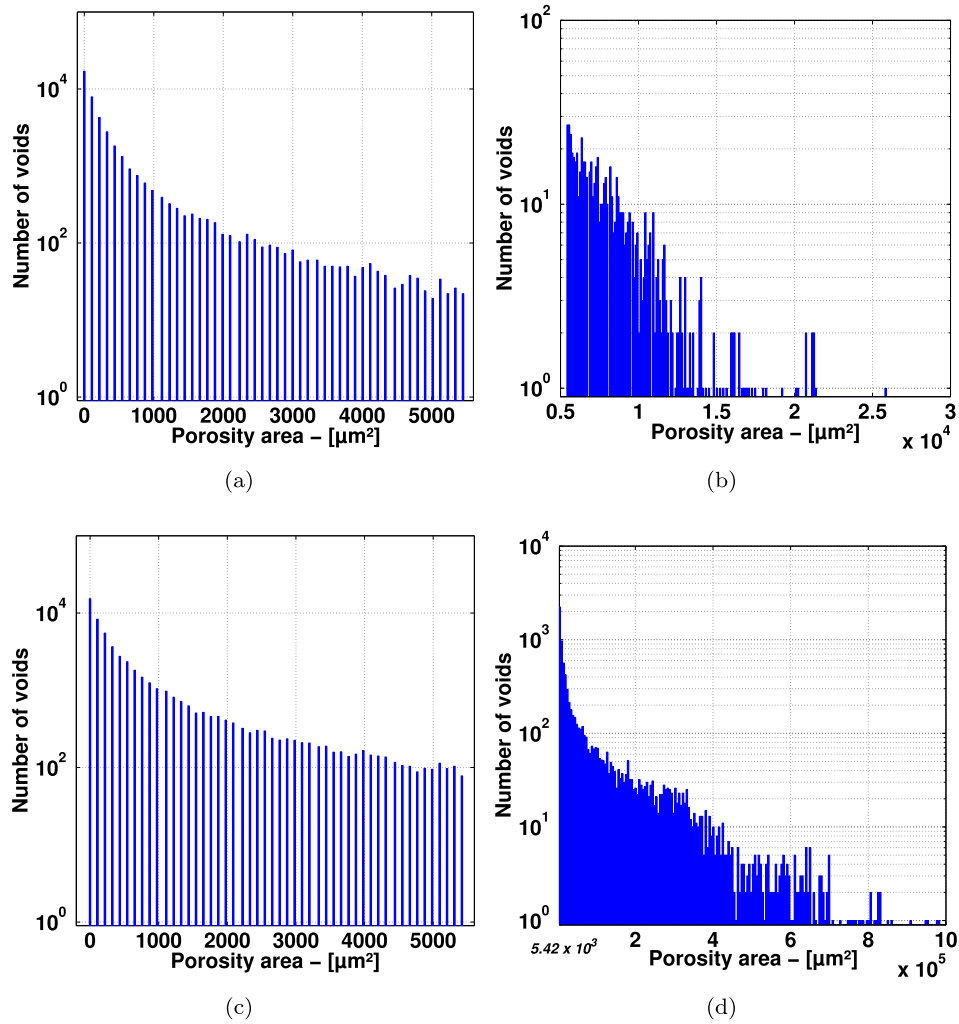


Fig. 12. 3D representation of porosities for commingled sample B4 ( $V_p = 12.11\%$ ). (For interpretation of the references to colour in this figure legend, the reader is referred to the web version of this article.)



**Fig. 13.** Void area distribution: (a) Sample B5 - Micro-voids ( $< 5.4 \times 10^3 \mu\text{m}^2$ ) - (b) Sample B5 - Macro-voids ( $> 5.4 \times 10^3 \mu\text{m}^2$ ) - (c) Sample B4 - Micro-voids ( $< 5.4 \times 10^3 \mu\text{m}^2$ ) - (d) Sample B4 - Macro-voids ( $> 5.4 \times 10^3 \mu\text{m}^2$ ). (For interpretation of the references to colour in this figure legend, the reader is referred to the web version of this article.)

distribution of micro-voids are quite similar between A3 and A5 samples. However, the number of *micro-porosities* is higher for sample A5 than for sample A3. Distribution graphs show larger macro-porosities for sample A5 in comparison with sample A3 which is confirmed by the CT-scans observation in Fig. 10 (b) and (d).

#### 4.1.2. Commingled fabric laminates

Void content (matrix digestion method) in commingled fabric laminates ranges from 1.65% to 12.11%. Mean ply thickness (0.328 mm) is significantly higher than the theoretical one (0.297 mm) and indicates a poor consolidation quality. Fiber volume ratio is around 55.0% for all commingled laminates except for B4 specimen with only 49.51%. This specimen exhibits the highest void content (12.11%) measured during this experimental study. Minimal void content is obtained with specimen B5 with a value of 1.65%.

Fig. 11 shows CT-scans of the commingled fabric laminates for three porosity levels. According to slices analysis, several void types are visible:

- **Inter-yarn voids:** These voids are located mostly between yarns or in contact to yarn surface. Their sizes are directly linked to the vacuum level and depend on consolidation parameters. For sample B4 which has the highest porosity level, these porosities agglomerate

into one macro void.

- **Intra-yarn voids:** Visible on sample B2 and B4, these voids are considered as micro-voids and have a spherical shape. The number of these porosities is lower than the inter-yarn ones.
- **Yarn cross failure:** Observed as cracks inside yarns in warp and weft direction with a length approximately equal to the minor axis of its cross section. These defects are parallel to fiber axis and are distributed uniformly in the laminate. They are found for all porosity levels. That suggests fiber/matrix de-cohesion inside yarns provoking transversal crack propagation. When compared to powdered laminates two tentative explanations can be given: First carbon fibers used during yarn manufacturing are sized. The sizing, developed for thermoset composites, are degraded at consolidation temperature and may generate volatiles that decreased the fiber-matrix bonding. On the contrary, these defects do not concern laminates using thermoplastic powdered semi-preg because fibers are not sized.

In the second explanation, transverse cracks are in general related to the internal stresses that are generated during temperature decrease after consolidation. In the commingled yarn, polymer filaments are used and it was known that filament processing step in air and at high temperature may degrade polymer quality and ductility [15–17].

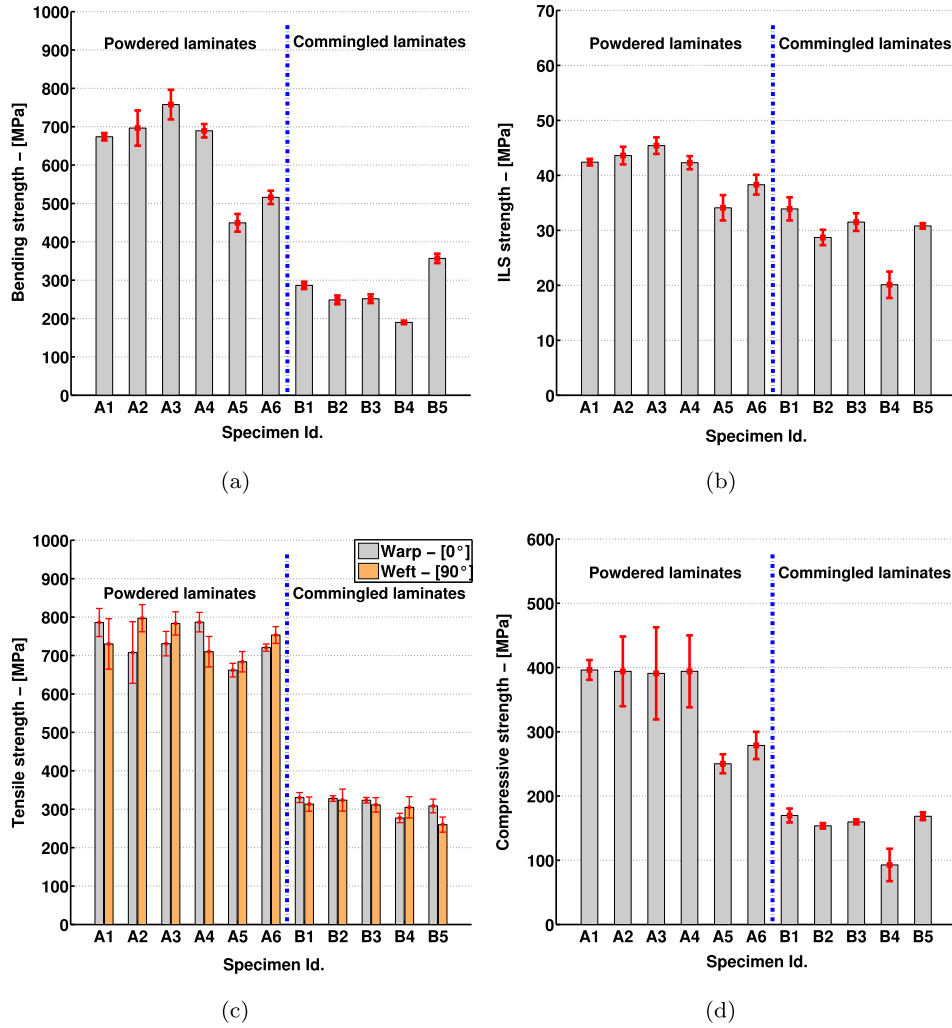


Fig. 14. Rupture strength of powdered and commingled laminates: (a) Three point bending - (b) ILSS - (c) Tensile in warp and weft direction - (d) Compressive. (For interpretation of the references to colour in this figure legend, the reader is referred to the web version of this article.)

A 3D representation of voids for sample **B4** is shown in Fig. 12. In contrary to the powdered case, voids look like macro-bubbles which are located between the plies. The 3D views suggest, in this case, the connection of these macro-voids in laminate thickness. Intra-yarn voids are also visible and in warp and weft direction of the reinforcement. Void area distribution for commingled laminates **B5** ( $V_p = 1.65\%$ ) and **B4** ( $V_p = 12.11\%$ ) are presented in Fig. 13. There is the same micro-void size distribution between these two samples. However, an increase of macro-void size with the void content is noticed with a maximal porosity area increased by a factor of 10.

Void observations performed for the two laminate types (powdered and commingled) show the importance of polymer integration strategy inside the textile reinforcement with respect to void formation, shape and consolidation conditions. Commingled laminate consolidation is more difficult than powdered one.

#### 4.2. Mechanical properties

Elastic moduli in bending, tension (warp and weft directions) and compression are shown in Fig. 15 for the two laminates. Moduli in tension are higher for powdered than comingled laminates with a respective average of 55.5 GPa (respectively standard deviation of 1.7 GPa) and 45.8 GPa (respectively standard deviation of 3.7 GPa). Values in compression are in the same order of magnitude with 55.3 GPa for

powdered fabric and 43.9 GPa for commingled fabric; however, a high standard deviation ( $>5.0$  GPa) was recorded. The higher modulus value of sample **A4** is related to the higher fibers volume fraction (59%). Moduli in bending are nearly constant for powdered laminates with a value of  $48.8 \text{ GPa} \pm 1.1 \text{ GPa}$  whereas modulus varies between 34.8 GPa and 45.6 GPa for commingled fabrics.

Rupture strength results for powdered and commingled laminates are reported in Fig. 14. It can be seen that laminates made of powdered fabrics show higher rupture strength values than commingled ones for all test conditions (bending, tensile, compressive and ILSS) even if commingled laminates have a higher fiber volume fraction (55%) than powdered laminates (50%). Tensile warp and weft rupture properties are close to each other for all laminates. Due to the stretch broken carbon fibers in the commingled laminates their tensile and compressive rupture stress are less than half of the powdered ones. These results show the same trend as those reported by Svensson [18] where stretch-broken carbon and polymer filaments induce a reduction of longitudinal strength and moduli.

#### 4.3. Influence of consolidation cycle on porosity level

In Fig. 16, external pressure values applied during laminate consolidation are related to void content and pressure level inside the bagging.

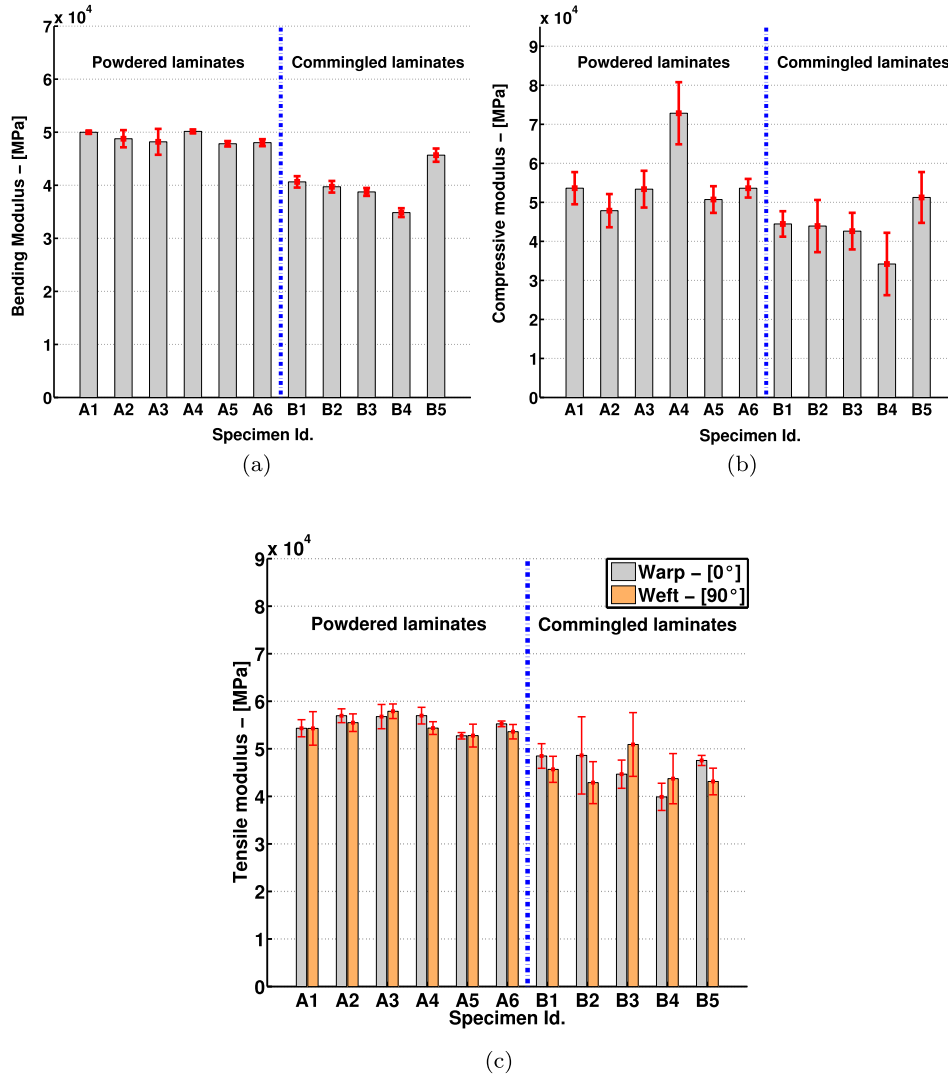


Fig. 15. Elastic moduli for powdered and commingled laminates: (a) Bending - (b) Compressive - (c) Tensile in warp and weft direction. (For interpretation of the references to colour in this figure legend, the reader is referred to the web version of this article.)

It appears that a higher external pressure ensures a better consolidation process in terms of void content. The trend is similar for the two types of semi-pregs but with different amplitudes. For the powdered fabric an increase of external pressure by 0.5 MPa contributes to a reduction by half of the void content (Laminate A1 versus A5). For the commingled system, there is a 30.0% decrease of the void content when the pressure rises by 0.7 MPa between laminate B1 and B2. Laminate B4 shows the highest void content measured in this experimental campaign despite an external pressure of 1.7 MPa. A vacuum loss occurred at the beginning of the manufacturing cycle and hindered the air evacuation.

Fig. 16 also shows that vacuum level helps significantly in void reduction for both fabrics. Vacuum applied inside the bagging improves the laminate quality by evacuating air and volatile particles trapped inside the textile reinforcement. A vacuum pressure maintained during the whole process limits the amount of porosity and their clustering inside the laminate and also improves the homogeneity of the whole part. It appears that powdered samples A1 (2.46%) and A3 (1.55%), manufactured with 0.5 MPa as external pressure and a pressure inside the bagging respectively maintained at +0.06 MPa and -0.01 MPa, have comparable void levels than sample A2 (2.45%) and A4 (2.27%) which were manufactured with respectively 1.2 MPa and 1.7 MPa and

no vacuum during the consolidation. Same observations are made for commingled fabrics in particular between sample B1 (6.02% and internal pressure maintained at +0.06 MPa) and sample B3 (7.09% and no air evacuation during the consolidation step) which were consolidated with the same external pressure 0.5 MPa.

Duration of consolidation step also contributes to void reduction during sheet manufacturing. For the powdered fabric, a higher value of this parameter (from 10 min to 20 min) results in a porosity level reduction of around porosity level of 3% which represents a void content reduction of 1.0% (Table 3) (Fig. 7) (Samples A5 and A6). Results for commingled fabric do not permit to establish the same conclusion due to the other involved factors ( $P_{applied}$ ,  $P_{vacuum}$ ). However, as well as for the external pressure, there is a limit [10–12 bars] where, beyond this value, the effect becomes negligible. An optimal value has to be found, taking into account the whole manufacturing time and the viscous behavior of the matrix.

An optimal combination of all these process parameters allows an improvement of laminate quality. The external pressure, as reported in Lystrup's [2] work, impacts strongly the porosity level. However, regarding the previous conclusions, composite part quality obtained after autoclave consolidation also depends strongly on the combination of external pressure and vacuum level (allowing air evacuation) inside the

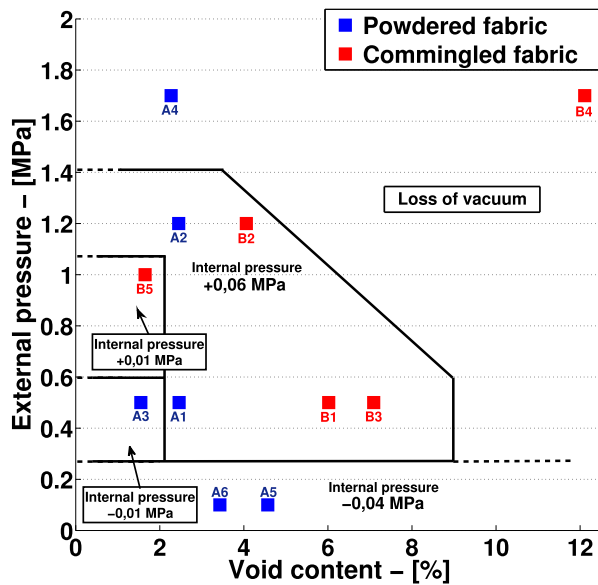


Fig. 16. Effect of consolidation pressure and pressure level inside the bagging on void content. (For interpretation of the references to colour in this figure legend, the reader is referred to the web version of this article.)

bagging. Liu [3] also underlines the need to maintain vacuum level with an external pressure in order to optimize the void content. Moreover with a vacuum pressure maintained during the entire process, the external pressure required to reach a low porosity level is lower. Duration at consolidation temperature also contributes to the void reduction but at a lower level.

#### 4.4. Mechanical properties in relation with void content

Voids have a significant impact on mechanical properties of C/PPS laminates manufactured with powdered and commingled prepreps. All mechanical properties (strength and moduli) decrease with void content. This drop depends on the type of mechanical test.

Mean rupture strength with respect to void content is plotted in Fig. 17 for powdered and commingled fabrics. For powdered fabric, bending and inter-laminar shear strengths decrease linearly with void content. The maximum value is reached for a void content of 1.55% with 757.6 MPa for bending strength and 45.4 MPa for ILSS. Tensile strength in warp [0°] and weft [90°] direction remain nearly constant until a porosity level of 3.5%. However, strength values for weft direction are slightly higher than warp direction values. Compressive rupture stresses are not affected by porosity level up to 2.5%. The maximum standard deviation is as high as 100 MPa especially for compressive stresses. For the commingled laminate, bending strength is the most sensitive to void content with a strength loss higher than 40.0% when void content increases from 1.0% to 12.0%. On the contrary, tensile strength values, in both directions, show a limited sensitivity to void content (decrease not higher than 20.0%). ILSS and compressive rupture stresses are nearly constant up to 7.0%.

Fig. 18a shows the moduli variations measured for bending, tensile and compressive tests as a function of void content for powdered fabric. There is a slight decreasing (less than 10%) for the tensile modulus in both testing directions when void content increases from 1.55% to 4.57%. The values stay in the range [52–58 GPa] with a maximum standard deviation of 2.5 GPa. The trend is similar for bending modulus with a value between 47.0 GPa and 51.0 GPa. The same trend is observed for compression. Nevertheless the standard deviation is higher (close to 2.0 GPa). The high value registered for sheet A4 ( $V_p = 2.27\%$ ) is attributed to the high fiber volume fraction due to matrix squeezing

during manufacturing.

As shown in Fig. 18b, bending and compressive moduli for the commingled fabric laminate are also sensitive to void content variation with respectively a loss of 22.0% and 30.0% when porosity increases from 1.0% to 12.0%. Tensile moduli, in warp and weft directions, decrease is limited to 20.0%. Nevertheless these latter results show a high standard deviation that may be partly related on one side to fiber orientation variation generated during the dry plain weave lay-up and on the other side to porosity variation from one sample to the other.

#### 4.5. Influence of void size and shape on mechanical properties

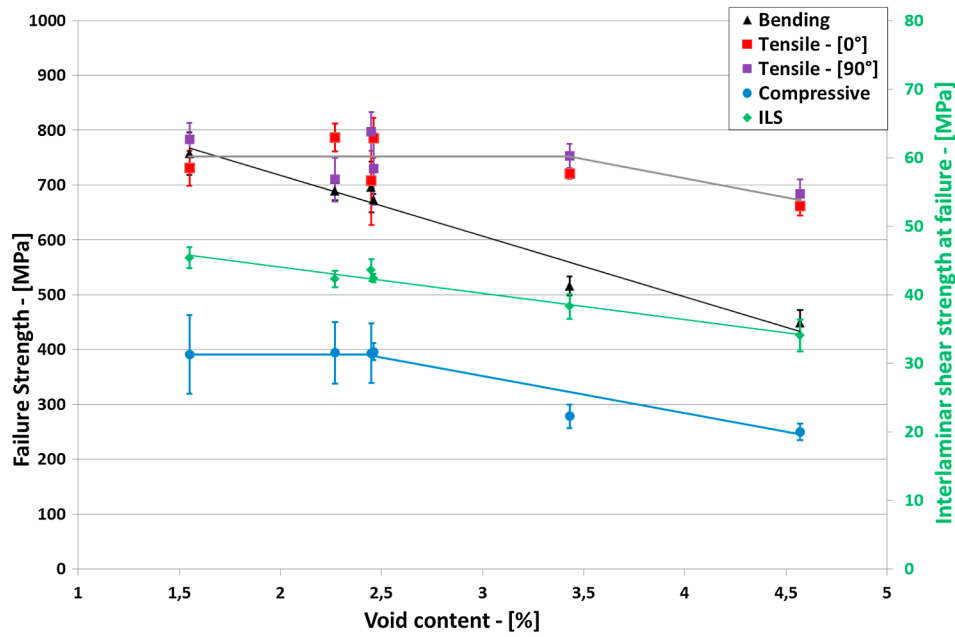
For both materials, mechanical properties, in particular failure strength, decrease with void content increase. However, as suggested by Lambert [19], this analysis remains too global and does not permit to understand fully the mechanical properties/porosity relationships. Size, orientation, localization of voids must be taken into account. To illustrate this aspect, bending strength mechanical properties are considered.

For the powdered laminates, voids are clusters inside warp and weft yarns as seen in Fig. 8. These intra-yarn voids grow with void content and have the potential to become multiple sites for crack initiation and propagation [19,20]. In Fig. 19, bending failure modes of specimen A2 and A5 illustrate the failure mode dependency for two porosity levels. Tensile and compressive fiber failures occur for a void content of 1.55% A2 with a bending strength as high as 757.6 MPa (Fig. 17a). On the contrary, elongated interlaminar cracks are observed in specimen A5 with a void content of 4.57% and bending failure strength as low as 449.5 MPa. Void area distribution reported in Fig. 10 shows a higher amount of macro-porosities in specimen A5 than specimen A2. Related to CT-scan images in Fig. 8, voids may be considered as active sites for crack propagation which induce interlaminar delamination failure mode in the plies. Bending stress-strain curves for increasing void content are plotted in Fig. 20a; they confirm a change in rupture mode if porosity level is higher than 3.0%.

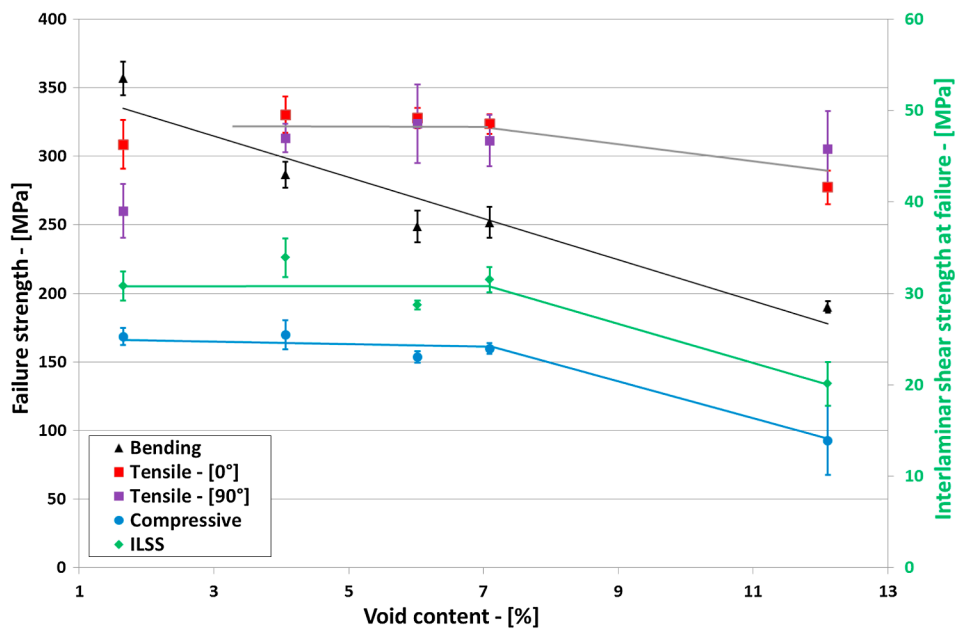
For commingled laminates, most voids are located between yarns as can be seen in Fig. 11. They become larger with a more elongated shape as the void content increases which is confirmed by void area distribution reported in Fig. 13. They are also preferentially oriented in warp and weft direction of textile reinforcement. In specimen B4 with a 12.11% void content, these voids permit crack propagation between the plies (interlaminar propagation) (Fig. 21 (a)) and explain the important decrease of bending failure strength value (190.0 MPa) whereas specimen B5 ( $V_p = 1.65\%$ ) shows a localized bending failure strength of 356.7 MPa (Fig. 22 (a)). Bending stress-strain curves of commingled laminates (Fig. 20b) are significantly different from those observed for powdered laminate samples. After an initial quasi-linear part until reaching the maximal bending stress there is no sample rupture with a stress drop, but a smooth decrease followed by a nearly constant plateau value up to high strains. This is related to the interlaminar rupture mode that happens for this type of laminate manufactured from commingled fabrics. Inter-ply porosities are considered as active for crack initiation and propagation and impact significantly the rupture mode when void content is higher than 3.0%. Failure modes are presented for samples B4 (Fig. 21 (b)) and B5 (Fig. 22 (b)). Both figures show micro-buckling failures in the compressive failure area. However, inter and intralaminar cracks, observed for sample B4, confirm the impact of inter-ply voids on the failure mode and the diminution of failure stress in bending, compressive and interlaminar shear (Fig. 14).

## 5. Conclusion

C/PPS composite laminates were manufactured from powder impregnated and commingled yarns prepreg fabrics. Consolidation cycles were defined to obtain laminates with a porosity level within the range 1.0–13.0%.



(a)



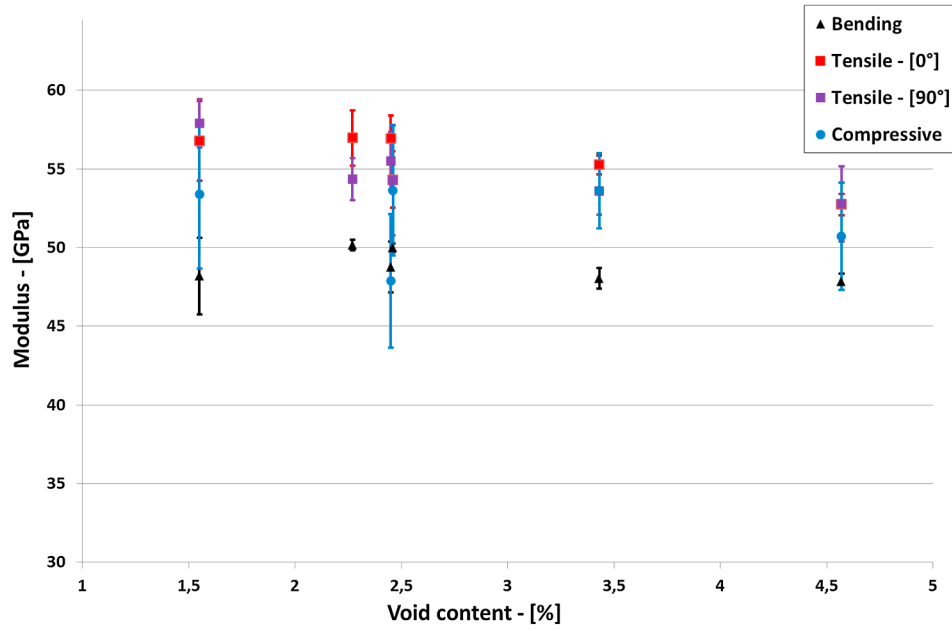
(b)

Fig. 17. Evolution of failure strength properties: (a) Powdered laminates - (b) Commingled laminates. (For interpretation of the references to colour in this figure legend, the reader is referred to the web version of this article.)

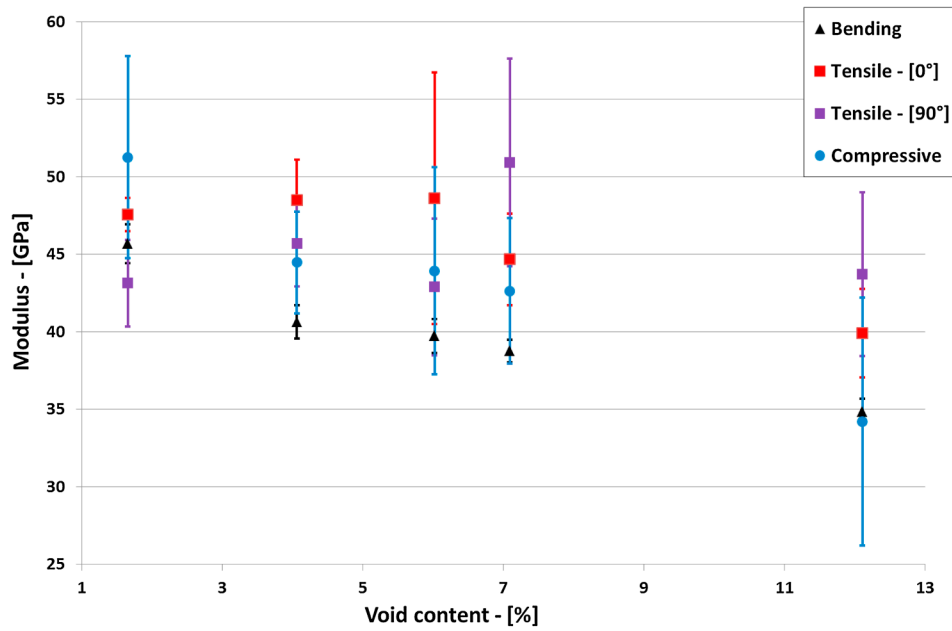
Consolidation pressure impacts considerably the quality of the composite parts. By raising the external pressure by 0.5 MPa, the void content decreases from 7.0% to 1.65% for commingled system and from 4.60% to 2.50% for powdered system. A first pressurization (as a first step of 0.5 MPa) of the lay-up also contributes to the defect reduction and prevents the bagging break. The decrease of the internal pressure in the laminate before the consolidation step significantly increases the void content. A maintained low pressure inside the bagging during the whole process ensures the consolidation of the laminate with an acceptable

porosity level in accordance with aeronautic standards. It also improves the homogeneity in terms of defects in the laminate. Consolidation duration impacts to the composite part quality by decreasing slightly the void content when it increases.

Mechanical properties of laminates manufactured from powdered fabrics show higher mechanical properties than those manufactured from stretch broken commingled fabrics whatever the void content. Experimental results show a dependency of mechanical properties in terms of failure strength to void content. It appears that inter-laminar



(a)



(b)

**Fig. 18.** Elastic moduli variation: (a) Powdered laminates - (b) Commingled laminates. (For interpretation of the references to colour in this figure legend, the reader is referred to the web version of this article.)

shear and bending strength are the most sensitive to void level when compared to tensile strength in warp and weft orientation. Moduli are slightly affected by void content variation for powdered laminates except for commingled laminate moduli with a minimal reduction of 20.0% (obtained for modulus in tension) when void content increases from 1.0% to 12.0%. In addition, it has been noticed that porosity size, shape and location impact mechanical properties. For powdered laminates, the cluster of void changes the failure mode in bending. For commingled laminates, inter yarn voids modification in size and shape

explain mechanical behavior change.

The identification of process parameters which have the biggest impact on the laminates microstructure allows the optimization of consolidation cycle. The use of commingled fabrics with stretch broken fibers offers the possibility to produce by consolidation thermoplastic composite parts with complex shapes contrary to powdered fabrics. Further studies has to be done in order to optimize the consolidation cycle thanks to the mechanical polymer behaviour.

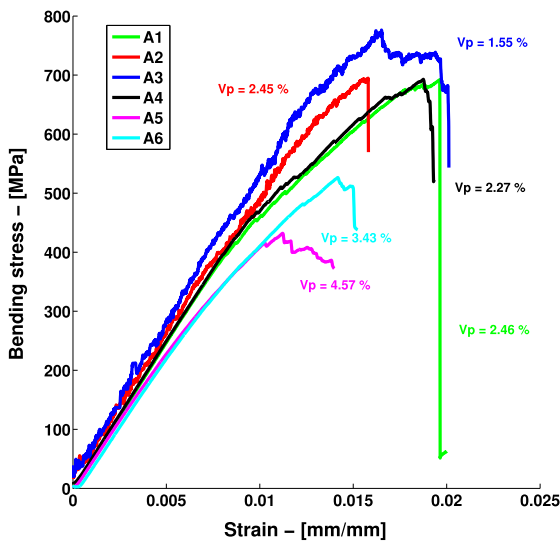


(a)

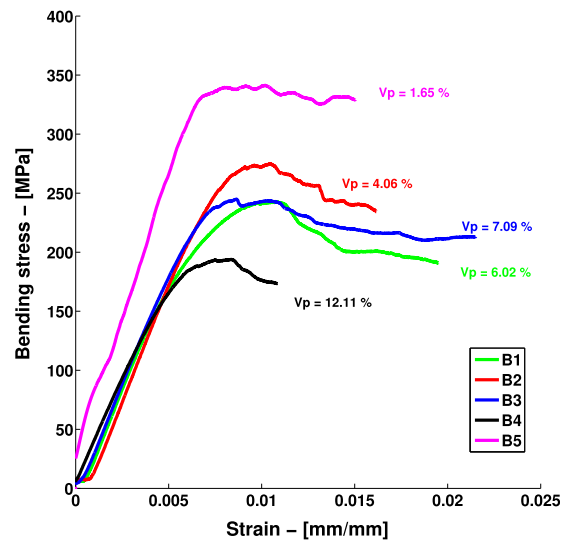


(b)

**Fig. 19.** Bending failure mode for powdered laminate: (a) Specimen A2 - (2.45%) (b) Specimen A5 - (4.57%). (For interpretation of the references to colour in this figure legend, the reader is referred to the web version of this article.)



(a)

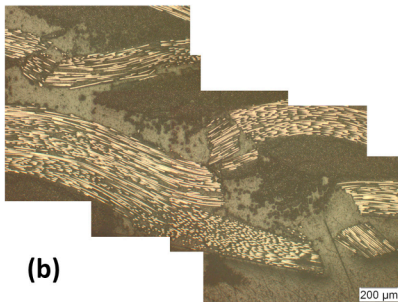


(b)

**Fig. 20.** Bending stress–strain curves with respect to void content: (a) Powdered laminates - (b) Commingled laminates. (For interpretation of the references to colour in this figure legend, the reader is referred to the web version of this article.)



(a)

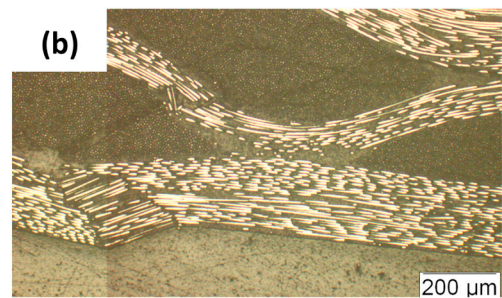


(b)

**Fig. 21.** Bending failure mode for commingled laminate B4 (12.11%): (a) macro observation - (b) micrography ( $\times 100$ ). (For interpretation of the references to colour in this figure legend, the reader is referred to the web version of this article.)



(a)



(b)

**Fig. 22.** Bending failure mode for commingled laminate B5 (1.65%): (a) macro observation - (b) micrography ( $\times 100$ ). (For interpretation of the references to colour in this figure legend, the reader is referred to the web version of this article.)

## Acknowledgement

This work was supported by BPI France and Region Midi-Pyrénées in the frame of ACAPULCO project.

## References

- [1] Klinkmüller V, Um MK, Steffens M, Friedrich K, Kim BS. A new model for impregnation mechanisms in different GF/PP commingled yarns. *Appl Compos Mater* 1994;1:351–71. <https://doi.org/10.1007/BF00568041>.
- [2] Lystrup A, Andersen TL. Autoclave consolidation of fibre composites with a high temperature thermoplastic matrix. *J Mater Process Technol* 1998;77(1-3):80–5. [https://doi.org/10.1016/S0924-0136\(97\)00398-1](https://doi.org/10.1016/S0924-0136(97)00398-1)<http://www.sciencedirect.com/science/article/pii/S0924013697003981>.
- [3] Liu L, Zhang B-M, Wang D-F, Wu Z-J. Effects of cure cycles on void content and mechanical properties of composite laminates. *Compos Struct* 2006;73(3):303–9. <https://doi.org/10.1016/j.compstruct.2005.02.001><http://www.sciencedirect.com/science/article/pii/S0263822305000437>.
- [4] Ledru Y, Bernhart G, Piquet R, Schmidt F, Michel L. Coupled visco-mechanical and diffusion void growth modelling during composite curing. *Compos Sci Technol* 2010;70(15):2139–45. <https://doi.org/10.1016/j.compscitech.2010.08.013><http://www.sciencedirect.com/science/article/pii/S0266353810003210>.
- [5] Zhu H-y, Li D-h, Zhang D-x, Wu B-c, Chen Y-y. Influence of voids on interlaminar shear strength of carbon/epoxy fabric laminates. *Trans Nonferr Metals Soc China* 2009;19:s470–5. [https://doi.org/10.1016/S1003-6326\(10\)60091-X](https://doi.org/10.1016/S1003-6326(10)60091-X)<http://www.sciencedirect.com/science/article/pii/S100363261060091X>.
- [6] de Almeida SFM, dos Santos Nogueira Neto Z. Effect of void content on the strength of composite laminates. *Compos Struct* 1994;28(2):139–48. [https://doi.org/10.1016/0263-8223\(94\)90044-2](https://doi.org/10.1016/0263-8223(94)90044-2)<http://www.sciencedirect.com/science/article/pii/0263822394900442>.
- [7] Ye L, Klinkmuller V, Friedrich K. Impregnation and Consolidation in Composites Made of GF/PP Powder Impregnated Bundles. *J Thermoplast Compos Mater* 1992;5(January):32–48. <https://doi.org/10.1177/089270579200500103>.
- [8] Olivier P, Cottu JP, Ferret B. Effects of cure cycle pressure and voids on some mechanical properties of carbon/epoxy laminates. *Composites* 1995;26(7):509–15. [https://doi.org/10.1016/0010-4361\(95\)96808-J](https://doi.org/10.1016/0010-4361(95)96808-J).
- [9] Santulli C, Brooks R, Rudd CD, Long aC. Influence of microstructural voids on the mechanical and impact properties in commingled E-glass/polypropylene thermoplastic composites. *Proc I MECH E Part L J Mater:Des Appl* 2002;216(2):85–100. <https://doi.org/10.1243/146442002320139298>.
- [10] Bernet N, Michaud V, Bourban P-E, Månson J-A. Commingled yarn composites for rapid processing of complex shapes. *Compos Part A: Appl Sci Manuf* 2001;32(11):1613–26. [https://doi.org/10.1016/S1359-835X\(00\)00180-9](https://doi.org/10.1016/S1359-835X(00)00180-9)<http://www.sciencedirect.com/science/article/pii/S1359835X00001809>.
- [11] Bourban P-E, Bernet N, Zanetto J-E, Månson J-AE. Material phenomena controlling rapid processing of thermoplastic composites. *Compos Part A: Appl Sci Manuf* 2001;32(8):1045–57. [https://doi.org/10.1016/S1359-835X\(01\)00017-3](https://doi.org/10.1016/S1359-835X(01)00017-3)<http://www.sciencedirect.com/science/article/pii/S1359835X01000173>.
- [12] Fernández I, Blas F, Frövel M. Autoclave forming of thermoplastic composite parts. *J Mater Process Technol* 2003;143-144:266–9. [https://doi.org/10.1016/S0924-0136\(03\)00309-1](https://doi.org/10.1016/S0924-0136(03)00309-1).
- [13] Little JE, Yuan X, Jones MI. Characterisation of voids in fibre reinforced composite materials. *NDT & E Int* 2012;46:122–7. <https://doi.org/10.1016/j.ndteint.2011.11.011><http://linkinghub.elsevier.com/retrieve/pii/S0963869511001769>.
- [14] Rasband W. Image processing and analysis in Java (ImageJ); 2014. <<http://imagej.nih.gov/ij>> .
- [15] Peters OA, Still RH. The thermal degradation of poly(phenylene sulphide)part 1. *Polym Degrad Stabil* 1993;42(1):41–8. [https://doi.org/10.1016/0141-3910\(93\)90023-C](https://doi.org/10.1016/0141-3910(93)90023-C)<http://www.sciencedirect.com/science/article/pii/014139109390023C>.
- [16] Lamethe JF. Adhesion study of semi-crystalline thermoplastic composites; application to the welding process, Theses, Université Pierre et Marie Curie - Paris VI, beauchêne Pierre (co-directeur); Dec. 2004. <<https://tel.archives-ouvertes.fr/tel-00008449>> .
- [17] Bessard E. Matériaux composites structuraux à base PEEK élaborés par thermo-compression dynamique: relation procédé-propriétés, Thèse, Université de Toulouse III - Paul Sabatier; 2012.
- [18] Svensson N, Shishoo R. Manufacturing of thermoplastic composites from commingled yarns - a review. *J Thermoplast Compos Mater* 1998;11:22–56. <https://doi.org/10.1177/089270579801100102>.
- [19] Lambert J, Chambers AR, Sinclair I, Spearing SM. 3D damage characterisation and the role of voids in the fatigue of wind turbine blade materials. *Compos Sci Technol* 2012;72(2):337–43. <https://doi.org/10.1016/j.compscitech.2011.11.023>.
- [20] Sisodia S, Garcea S, George A, Fullwood D, Spearing S, Gamstedt E. High-resolution computed tomography in resin infused woven carbon fibre composites with voids. *Compos Sci Technol* 2016;131:12–21. <https://doi.org/10.1016/J.COMPSCITECH.2016.05.010><http://www.sciencedirect.com/science/article/pii/S0266353816303542>.